Variable stiffness and damping components for semi-active vibration control and inflatable rigidization

Wang, Qinyu; Senatore, Gennaro; Jansen, Kaspar; Habraken, Arjan; Teuffel, Patrick

DOI
10.2749/manchester.2024.0534

Publication date
2024

Document Version
Final published version

Published in
Proceedings of the ABSE Symposium Manchester 2024

Variable stiffness and damping components for semi-active vibration control and inflatable rigidization

Qinyu Wang, Peng Feng
Key Laboratory of Civil Engineering Safety and Durability of China Education Ministry, Department of Civil Engineering, Tsinghua University, Beijing 100084, China

Gennaro Senatore
ILEK – Institute for Leightweight Structures and Conceptual Design, University of Stuttgart, Pfaffenwaldring 7 70569 Stuttgart, Germany

Kaspar Jansen
Department of Design Engineering, TU Delft, 2628 CE Delft, NL

Arjan Habraken, Patrick Teuffel
Chair of Innovative Structural Design (ISD), Department of Built Environment, TU Eindhoven, Eindhoven, the Netherlands

Contact: fengpeng@tsinghua.edu.cn

Abstract
The paper explores the potential applications of adaptive components based on shape memory polymer (SMP) composites in vibration control of plate/shell structures and rigidization of inflatable structures. These components achieve stiffness and damping variation by thermally actuating SMP between its glassy and rubbery states. In CASE A, steel-SMP sandwich plates of a truss bridge are actuated to glass transition temperature (Tg), where material damping reaches the peak to mitigate dynamic responses. CASE B proposes a simple and reversible rigidization method for inflatable structures, creating high compaction ratio and design flexibility. Converting the SMP layer between its glassy and rubbery states, inflatable structures achieve multiple functions during transportation, construction, and service life. Overall, adaptive components offer solutions to enhance structural performance and mitigate dynamic effects in demanding environments for various structures.

Keywords: adaptive components; shape memory polymer (SMP); variable stiffness and damping; vibration control; plate/shell structures; inflatable structures; physical rigidization; construction in extreme environments; structural performance; finite element analysis (FEA)

1 Introduction

1.1 Vibration control
Structural control strategies optimize performance in adaptive structures under changing loading conditions, categorized as passive, active, semi-active, and hybrid [1]. Passive systems, e.g. base isolation, require no control power but have limited capabilities. Active control effectively reduces structure responses, especially in seismic- [2] and wind-excited [3] buildings, but can be unstable due to high power density and control uncertainties. Semi-active control systems, like magnetorheological dampers, offer reliability and energy efficiency, but the non-linear control limits their applications in a particular objective and feedback law. Hybrid control combines passive,

semi-active, and active strategies but can be complex and costly to maintain [4, 5].

Adaptive structures counteract external loads through active control of internal forces and external geometry, offering better material utilization and lower whole-life energy compared to conventional passive structures [6]. Well-designed adaptive structures can achieve up to 70% savings compared to weight-optimized passive structures when the design is stiffness-governed [7]. Addressing the challenge of joint fixity during geometry reconfiguration is crucial as it impacts control accuracy, increases control effort, and may result in stress concentration. To address this challenge, our previous research proposes the use of adaptive joints with variable stiffness and damping properties to achieve flexibility during shape control. These joints utilize special materials, such as shape memory polymer (SMP), to achieve stiffness variation. By reducing stiffness and releasing the rotation degree of freedom, the joints transition from moment to pin connections [8]. An adaptive joint consists of a polyurethane-based SMP core reinforced by an SMP-Aramid skin, enabling stiffness and damping variation through thermally actuating SMP between its glassy and rubbery states. This transition phase increases material damping while reducing stiffness, resulting in frequency shift and enhanced structural damping [9]. Shake table tests on a 1/10 scale, 3-story frame prototype with 12 adaptive joints demonstrated significant improvements. By actuating adaptive joints, the structural damping ratio increased from 2.6% to 11.3%, and the first modal frequency shifted up to 37%. Under seismic excitation, notable reductions in top-story acceleration (43-50%) and base shear (35-51%) were achieved. The practical application of adaptive joints for vibration control in truss and frame structures has been successfully demonstrated [10, 9].

1.2 Inflatable rigidization

Construction in extreme environments, like extraterrestrial or polar locations, faces challenges from harsh conditions, limited resources, transportation obstacles, and labor shortages. The lunar surface exemplifies such extreme environments. The moon offers opportunities for scientific research, energy production, resource development, international cooperation, and commercial ventures, making lunar construction a cutting-edge field of immense scientific importance, driving advancements in human exploration and technology [11].

The lunar environment poses unique challenges for constructing lunar bases due to factors such as low gravity, ultra-high vacuum, large temperature variations, strong radiation, and limited resources. Inflatable structures have emerged as a highly promising and practical solution for designing lunar habitation modules, considering transportation, storage, construction, and reliability [12]. They are widely utilized in space capsule structures and offer significant advantages in lunar construction endeavors, such as lightweight, high packing efficiency, relatively low transportation costs, minimal on-site construction materials, and provision of a breathable environment [13, 14]. To enhance the long-term structural rigidity of inflatable structures, rigidization technologies are essential due to inevitable air leakage caused by permeability, connections, and punctures. Rigidized membrane structures offer advantages such as reduced reliance on continuous inflation, shape preservation even after punctures and air leakage, and improved structural safety, durability, and repairability. Defoort et al. classified rigidization technologies into three categories: mechanical, physical, and chemical rigidization. Among them, physical methods are commonly used due to their simplicity, reversibility, low energy requirements, shorter maintenance time, and allowing for ground testing and multiple applications [15]. SMPs fall under the physical category and possess desirable properties for inflatable lunar habitats, including high compaction rates, design flexibility, and simplified design. The special properties of SMPs make them very suitable for use in inflatable lunar habitats [16, 17]. SMPs can significantly reduce residual strains and stresses after deformation in deployable structures. However, the feasibility of large-scale lunar habitats is still under investigation.

This paper explores the extended applications of adaptive components comprised of SMP and its composites in plate/shell and inflatable structures. SMP is used for vibration control by actuating it to the viscoelastic region for enhancing damping, while inflatable rigidization employs the phase

transition of SMP from the rubbery to glassy state. In case A, a truss bridge equipped with SMP-steel plates under resonance and moving loads is explored numerically. The capability in dynamic response mitigation is verified. Case B, a flexible membrane comprised of aramid fiber fabric flexible resin, and SMP, is proposed for an inflatable lunar habitation module. This controllable and reversible rigidization technology strategically distributes SMP to form a well-shaped stiff endoskeleton and optimize material usage and activation energy. This adaptive stiff endoskeleton also aids in vibration control within the module, considering potential lunar dynamic excitations such as micrometeoroid impacts, moonquakes, or other vibrations [10].

1.3 Outline

This paper is arranged in sex sections. Section 2 introduces the principle and concept design of adaptive components. Sections 3 and 4 carry out two case studies to demonstrate the applications in vibration control of a truss bridge and rigidization of a semi-sphere inflatable structure. Sections 5 and 6 discuss and conclude the paper.

2 Variable stiffness and damping components

2.1 Conceptual design of adaptive joints

In our previous research, the adaptive joint is designed of an SMP core reinforced by an SMP-aramid skin. Figure 1 shows an example of this joint connected with columns and beams. Each joint incorporates a resistive heating wire embedded within the core [9, 10].

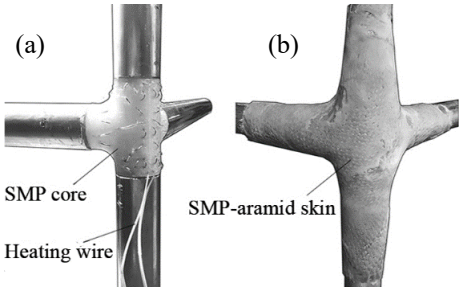

Figure 1. Adaptive joint: (a) SMP core with heating wire; (b) SMP-aramid reinforcement skin [10].

2.2 Material model

Dynamic mechanical analysis (DMA) measures the complex modulus, comprising storage modulus E' and loss modulus E''. E' represents energy stored in the elastic part, while E" accounts for heat dissipation due to friction. The $tan\delta$ ratio (E'/E'') indicates mechanical damping. With increasing temperature, the material undergoes a glassy to rubbery transition through a viscoelastic region, with a glass transition temperature of 65°C. During glass transition (50°C to 65°C), the elastic stiffness reduces by 96% while damping increases 11-fold.

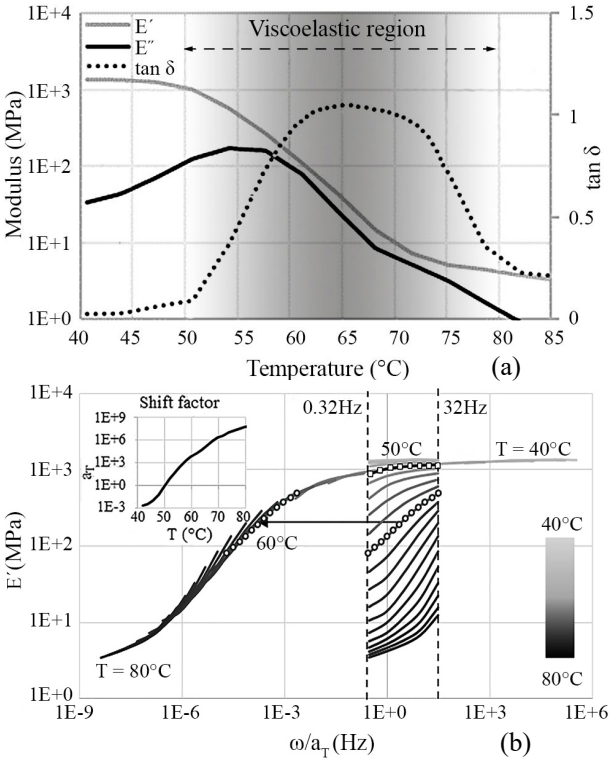

Figure 2. SMP material characterization through DMA: (a) storage modulus (E'), loss modulus (E"), and material damping (tan δ) vs. temperature at 1 Hz; (b) master curve [9].

Two SMP material models were developed for numerical analysis: thermoelastic and viscoelastic [9]. The thermoelastic model considers temperature-dependent behaviour, simplifying numerical simulations. The viscoelastic model accounts for time- and temperature-dependent properties, capturing stiffness and damping variations over time and temperature. In general, the thermoelastic model uses the storage modulus curve at 1 Hz (Figure 2(a)) and disregards viscoelastic damping effects. For the viscoelastic model, Experimental data obtained at different

temperatures and frequencies are mapped onto a master curve using the time-temperature superposition principle, as shown in Figure 2(b). The viscoelastic model is employed for a comprehensive analysis of dynamic response and performance evaluation of the proposed semi-active control strategy [9, 10]. A modulus of 8320 MPa and an ultimate stress of 107 MPa is assumed for the SMP-aramid reinforcement skin material based on experimental data.

3 Case A: vibration control of a pedestrian truss bridge

3.1 Conceptual design of adaptive plate elements

This paper explores the design of adaptive plate elements, where SMP is incorporated with metal plates. To validate the concept, a cantilever SMP-aluminium plate with dimensions of 5000mm x 1000mm x 50mm is designed for initial assessment, as depicted in
Figure 3. The initial damping ratio of the structure is set to 0 to isolate and quantify the increase in structural damping ratio solely due to material damping.

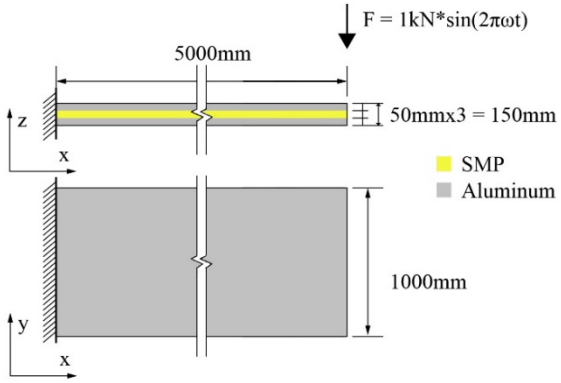

Figure 3. Adaptive SMP-aluminium sandwich plate.

The viscoelastic material model is employed for the plate in a full transient analysis, specifically a free vibration test, to assess the variation in damping due to viscoelastic effects. The damping ratio ζ is then computed through the displacement logarithmic decrement $\Delta = \ln(x_3(t)/x_3(t+1))$:

$$\zeta = \frac{\Delta/2\pi}{\sqrt{1+(\Delta/2\pi)^2}} \quad (1)$$

The frequency and damping vary as functions of temperature, as shown in Figure 4. By actuating the SMP layer from 25°C to glass transition temperature T_g=65°C, the frequency drops from 23Hz to 1.16Hz, reducing 27.8%, while the damping increases from 0 to 27.7%.

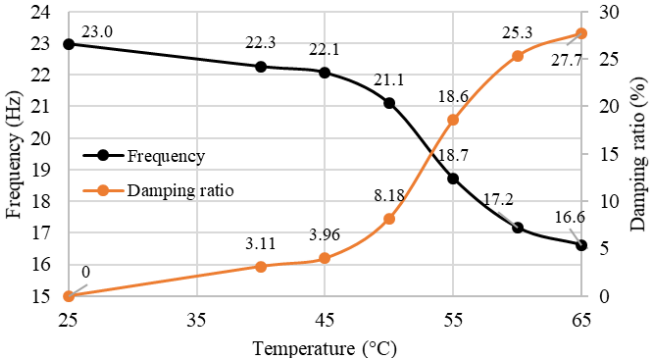

Figure 4. SMP-aluminium sandwich plate: frequency and damping ratio vs. temperature.

Dynamic response mitigation is verified under a resonance load F=1KN*sin(2πω) applied at the end of the beam, as shown in Figure 3. Actuating the SMP layer to 65°C reduces peak deformation by 90.6% (from 16.7 g to 1.49 g) and peak acceleration by 73.2% (from 9.19 mm to 2.46 mm) at the free end. This result confirms the applicability of the concept for vibration control in plate or shell structures, including curved surfaces. Further analysis is presented in later sections.

3.2 Truss bridge: structural design and FEM model

The studied structure is a simply supported planar truss footbridge with a 10m span, 2m width, and 0.5m rise, as shown in Figure 5(a). It features five SMP-steel sandwich panels installed at the top chords. The finite element model comprises beam elements (BEAM188) for the chords and bracings, and solid elements (SOLID186) for the sandwich plates. Figure 5(b) shows the finite element mesh with material and section information. Structural steel S355 is used for the beams and steel layers. The top chords and connection beams are H-shaped profiles with dimensions of 100mm x 68mm, 4.5mm web thickness, and 7.6mm flange thickness. The bottom chords have square hollow sections of 60mm x 60mm with a 3.2mm wall thickness, while other connection beams have square hollow sections of 30mm x 30mm with a 2mm wall thickness. The bridge geometry is meshed with solid elements of approximately 100mm for the SMP and 200mm for the steel

layers, and beam elements of 400mm length. Various analyses are conducted, including static analysis under a distributed live load, transient analysis with mode superposition for uncontrolled cases, and full transient analysis using the viscoelastic material model to assess the dynamic response under a moving load for controlled cases. The simulations are performed in Ansys Workbench. In each analysis, the adaptive components are actuated through resistive heating from ambient 25°C to T_g 65°C.

3.3 Static analysis

During static analysis, the top plates are subjected to a uniformly distributed live load with an intensity of 350 kg/m^2. When the SMP layer in the sandwich plate is actuated from 25°C to 65°C, the maximum static deformation of the structure increases from 24.2 mm to 26.9 mm, and the maximum combined stress of beams increases from 199MPa to 201MPa, within the allowable ranges.

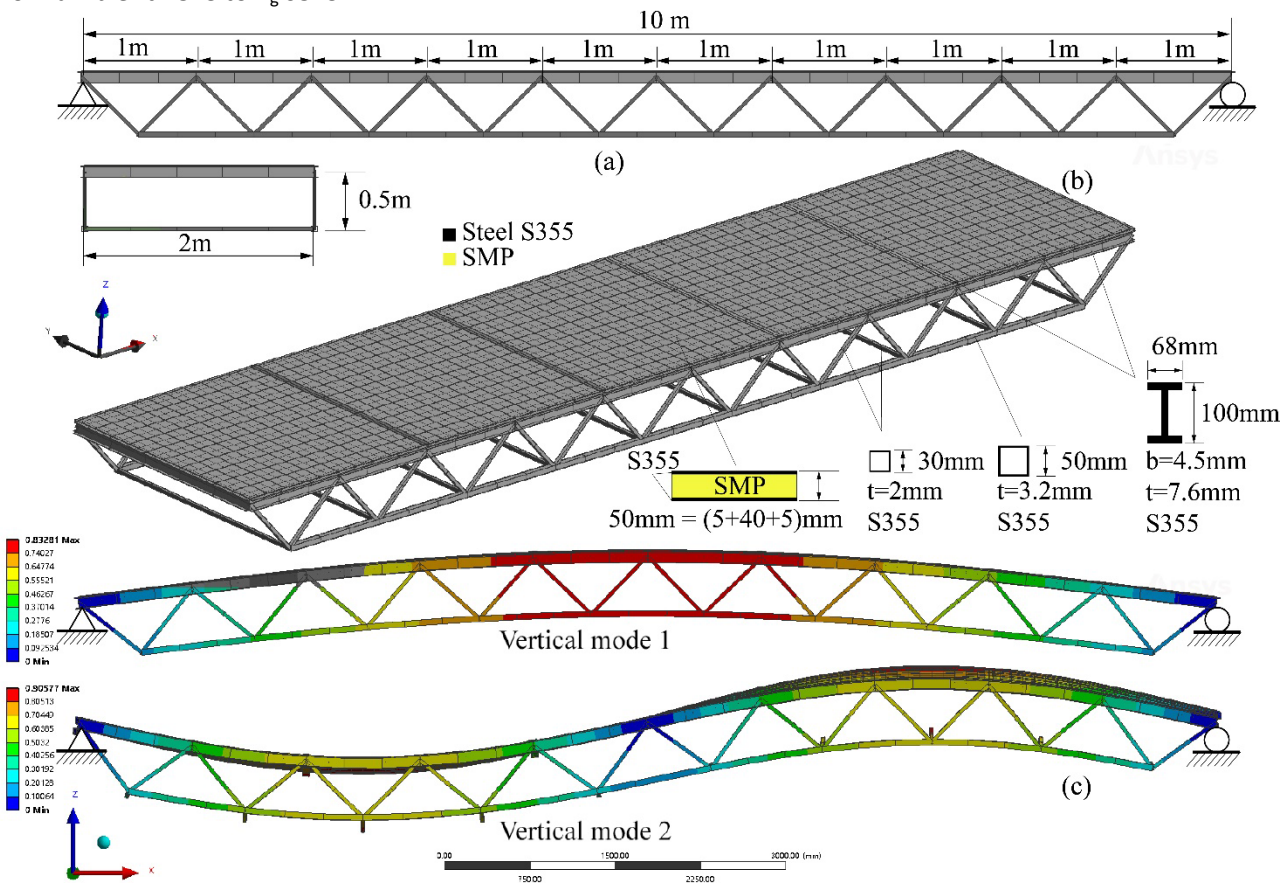

Figure 5. Truss bridge: (a) dimensions and support conditions; (b) finite element mesh with material and section information; (c) first and second vertical modal shapes.

3.4 Stiffness and damping variation

This section focuses on the separate study of two effects resulting from variations in joint stiffness: frequency shift and damping variation. Similar to Section 3.1, the frequency and damping variations over temperature are presented in **Error! Not a valid bookmark self-reference.**. When the SMP layer is actuated to 65°C, the first modal frequency drops 3.4%, while the damping increases from 0 to 0.69%.

Table 1. Frequency and damping vs. temperature

	25°C	40°C	50°C	55°C	60°C	65°C
f_1(Hz)	6.77	6.77	6.76	6.75	6.69	6.54
f_2(Hz)	20.91	20.87	20.80	20.46	19.39	16.72
S_{f1}(%)	-	0	0.15	0.30	1.18	3.40
S_{f2}(%)	-	0.19	0.53	2.15	7.27	20.04
ζ_1(%)	-	-	0.05	0.13	0.22	0.69

3.5 Vibration control under resonance load

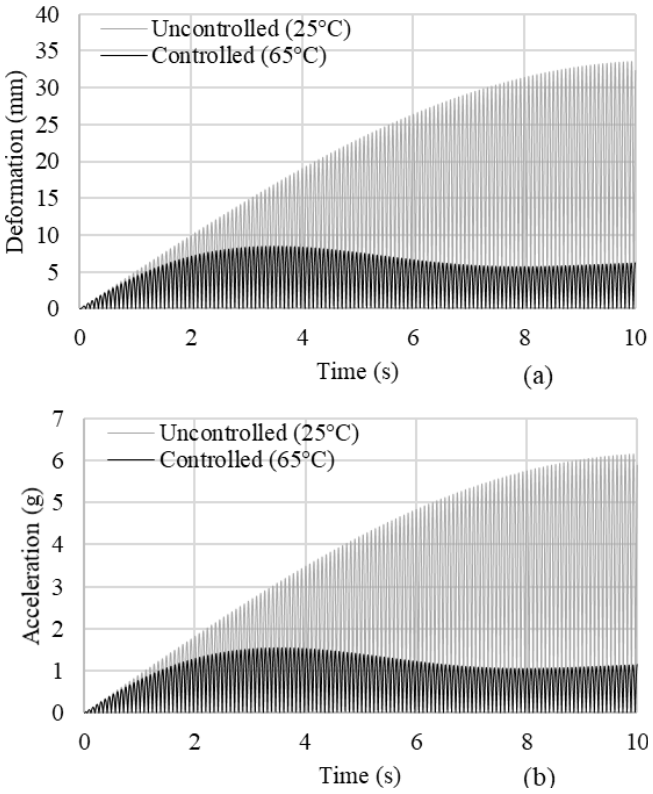

Figure 6. Truss bridge: (a)average deformation and (b) acceleration under resonance excitation.

By actuating the SMP to the controlled state, the deformation and acceleration peaks decrease by 70.4% (from 33.6mm to 9.95mm) and 74.8% (from 6.15g to 1.55g), respectively. The maximum combined stress in the beams decreases from 330MPa to 81MPa. Note that the dynamic responses will continue to increase until structural failure occurs without control. This verifies that even minor frequency shifts and damping increases can effectively prevent structural resonance.

3.6 Vibration control under moving load

In the conducted test, a moving load of 350 kg/m² was applied to each top plate, traversing from one side to the other and then reversing, at a speed of 1.4 m/s (walking pace). To simulate the transition between elements, the load intensity varied from 0 to 350 kg/m² as it approached the middle of the 2m x 2m plate and then decreased to 0 towards the end. However, the control results of this case did not yield the desired outcome, as the peak values of average acceleration and deformation remained nearly unchanged at both 25°C and 65°C. This observation can be explained by considering the bridge's first vertical modal frequency of 6.77Hz, which satisfies the criteria for human-induced vibration comfort based on the provisions outlined in BS 5400. According to these specifications, when the fundamental frequency of the superstructure exceeds 5Hz, the likelihood of vibration discomfort for pedestrians, whose typical frequency range falls between 1.6Hz and 2.4Hz, is minimal. Therefore, in this case, implementing vibration control measures is unnecessary.

An extra 10x = 14m/s moving load (typical car speed on residential roads 50km/h) is applied to the bridge for 14s. The average deformation and acceleration reach the peak within 1s, as shown in Figure 8. Regarding peak values, when the SMP is actuated, the deformation and acceleration change minor, from 13.1mm to 11.6mm and 2.19g to 1.99g, respectively. However, the later vibration amplitudes damp quickly to around 50%. Therefore, for future scenarios, it would be advisable to explore more extreme loads and intense vibration conditions, such as long-term vibration, resonance, and earthquakes.

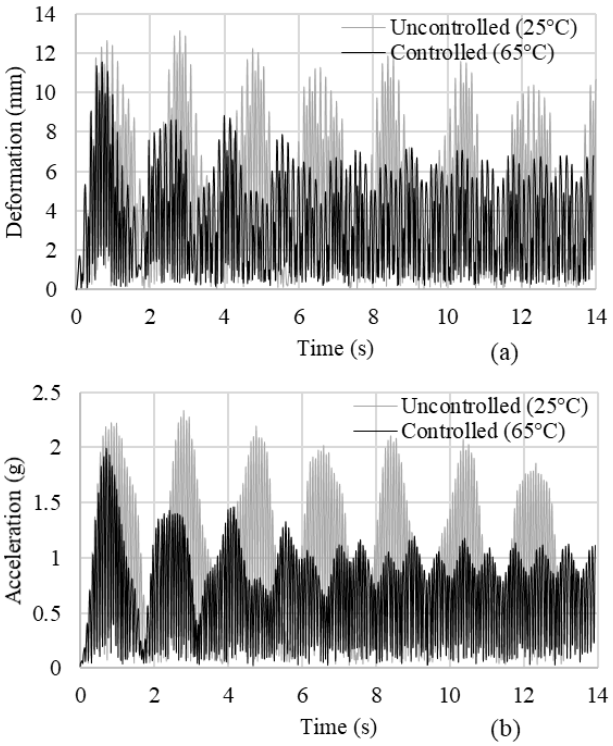

Figure 7. Truss bridge: (a)average deformation and (b) acceleration under 10x moving load.

4 Case B: Inflatable Rigidization of a semi-sphere inflatable habitat

4.1 Concept of rigidizable inflatable habitat

This paper proposes self-rigidizable lunar habitats comprised of 1) an inner inflatable structure providing living and research spaces for astronauts and 2) an outer regolith layer (regolith bricks or bags) for radiation protection, thermal insulation, and micrometeoroid impact resistance. To enhance membrane stiffness, a flexible AFRP composed of aramid (Kevlar) fiber and flexible resin handles tension. SMP or SMPC are manipulated to increase the stiffness of the inflatable structure, enabling it to meet various requirements during transportation, construction, and service. The construction process of self-inflatable lunar habitats includes inflation and expansion, rigidization, regolith coverage, and pressurization. In the rubbery state, SMP allows for easy folding of the membrane, while in the glassy state, it maintains the folded shape tightly for stowage and transportation. When SMP is actuated to the rubbery state again, the membrane becomes flexible and can be inflated and erected. Then, SMP enters the glassy state again, and the structure maintains the inflated shape. This rigidization process is reversible. Structures requiring multiple deployments can be folded and reused by actuating SMP above T_g, enabling cycles of folding and inflation. Inflatable lunar habitats incorporate a regolith layer to cover the rigidized structure, and the interior space is pressurized to 1 atm for human activities.

4.2 Static analysis: nonrigid vs. rigidized

To assess the rigidization effect, a 6m diameter semi-sphere inflatable structure is proposed. The membrane comprises a 5mm SMP layer and a 5mm AFRP resistance layer responsible for load-bearing. The FEM model incorporates SOLID186 elements for the SMP layer and SURF156 elements for AFRP's membrane effect. The mesh size for all elements is set at 200mm. The simulation assumes fixed support at the edge of the structure, neglecting considerations for foundation and anchoring factors. The main material properties used are based on previous research, as outlined in Table 2 [9]. Note that a small value of "1MPa" is assigned to the nonrigid SMP to simulate a membrane without rigidization.

Table 2. Main material properties [9]

	SMP nonrigid	SMP rigid	AFRP
Density (kg/m^3)	1050	1050	1451
Modulus (MPa)	1	1541	8321
Tensile strength (MPa)	-	40	300

In this static analysis, an inner pressure of 0.1 MPa (P_1) and an external pressure of 0.044 MPa (P_2) from a 3m regolith shielding layer are considered [18]. The support and loading conditions are shown in Figure 9(a). The structure, initially made of nonrigid SMP material, experiences a maximum deformation of 18.4 mm and a maximum equivalent (von Mises) stress of 55 MPa in the AFRP material. After rigidization, the maximum deformation decreases to 5.8 mm (reduced by 68%), and the maximum stress drops to 16MPa (reduced by 70.6%). Figure 9(b) and (c) compare the contour plots of nonrigid and rigid cases.

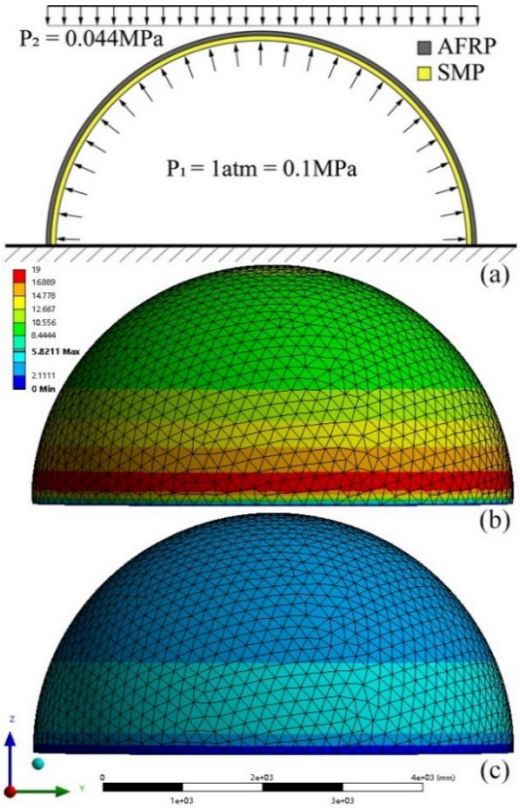

Figure 8. Semi-sphere inflatable habitat: (a) support and loading conditions; deformation at (b) nonrigid and (c) rigidized cases.

4.3 Air leakage

When punctures occur, the external pressure (P_2) decreases to zero while the internal pressure (P_1) remains constant, resulting in structural collapse (Figure *10*(a)). When the inner pressure drops to 0.005MPa, similar to the external pressure, the structure experiences sudden buckling and fails to converge due to excessive deformation. In the rigidized structure after air leakage (P_2 = 0), the maximum deformation and equivalent stress in the AFRP material are controlled at 5.9 mm and 14 MPa, respectively, demonstrating the effectiveness of the rigidizable layer in preventing collapse.

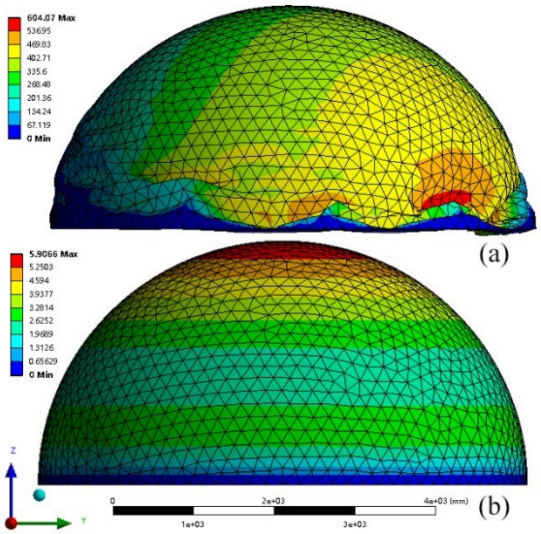

Figure 9. Semi-sphere inflatable habitat under air leakage: (a)nonrigid (collapse occurs) and (b)rigidized cases.

5 Discussion

Through two case studies, this study explores the application of adaptive components in vibration control of plate/shell structures and rigidization of inflatable structures. It is proven that the variable stiffness and damping components are effective in dynamic response mitigation a truss bridge equipped with SMP-metal plates and in preventing collapse of a semi-sphere inflatable structure after air leakage. However, the following notes are made here:

- In Case A, the effectiveness of this control strategy in managing a moving load of 1.4 m/s (typical walking speed) is limited. This is because in structural design, when the first vertical modal frequency of a bridge exceeds 5 Hz, human-induced vibration comfort (e.g., acceleration) is automatically considered satisfactory according to various design codes. Consequently, vibration control is not deemed necessary in such cases. Therefore, for future scenarios, it would be advisable to explore more extreme loads and intense vibration conditions, such as resonance and earthquakes.
- SMP integration into bridge panels shows more minor changes in stiffness and damping compared to its previous application in truss bridge joints. Despite increased SMP usage, the effectiveness is weaker than adaptive joints under resonance and moving loads. Future research is needed to optimize the form and arrangement of variable stiffness components.
- Regarding inflatable rigidization, anchoring issues and boundary conditions in inflatable structures require further design considerations.
- After air leakage, the membrane in the rigidized structure undergoes compression stress (up to 3.7 MPa at the support). Therefore, it is crucial to verify the optimal design and compressive performance of the rigidization layer.
- Thermal, radiation, and dynamic performances require future studies considering extreme lunar environments.

6 Conclusion

In conclusion, with good design, adaptive components with variable stiffness and damping show significant benefits in vibration control and shape control in various types of structures, including truss, frame, plate, shell, and inflatables. Their applications span civil engineering, mechanical engineering, robotics, aerospace, and other related fields.

7 Acknowledgements

This research project has been supported by National Natural Science Foundation of China (52308265).

8 References

[1] T. T. Soong and B. F. Spencer, "Active, semi-active and hybrid control of structures," *Bulletin of the New Zealand Society for Earthquake Engineering,* vol. 33, no. 3, pp. 387-402, 2000.

[2] B. F. Spencer Jr, R. E. Christenson and S. J. Dyke, "Next generation benchmark control problem for seismically excited buildings," in *Proceedings of the Second World Conference on Structural Control*, Kyoto, 1998.

[3] J. N. Yang, A. K. Agrawal, B. Samali and J. C. Wu, "Benchmark problem for response control of wind-excited tall buildings," *Journal of Engineering Mechanics,* vol. 130, no. 4, pp. 437-446, 2004.

[4] P. S. Harvey Jr, H. P. Gavin, J. T. Scruggs and J. M. Rinker, "Determining the physical limits on semi-active control performance: a tutorial," *Structural Control and Health Monitoring,* vol. 21, no. 5, pp. 803-816, 2014.

[5] G. Kınay and G. Turan, "A hybrid control of seismic response by passive and semi-active control strategies," *Journal of Engineering Science and Design,* vol. 2, no. 1, pp. 27-36, 2012.

[6] G. Senatore, P. Duffour and P. Winslow, "Synthesis of Minimum Energy Adaptive Structures," *Structural and Multidisciplinary Optimization,* vol. 60, no. 3, pp. 849-877, 2019.

[7] G. Senatore, P. Duffour and P. Winslow, "Exploring the Application Domain of Adaptive Structures," *Engineering Structures,* vol. 167, pp. 608-628, 2018b.

[8] Q. Wang, G. Senatore, K. Jansen, A. Habraken and P. Teuffel, "Multi-scale experimental testing on variable stiffness and damping components for semi-active structural control," *Composite Structures,* vol. 281, p. 114976, 2022.

[9] Q. Wang, G. Senatore, K. Jansen, A. Habraken and P. Teuffel, "Design and characterization of variable stiffness structural joints," *Materials & Design,* vol. 187, p. 108353, 2020.

[10] Q. Wang, G. Senatore, K. Jansen, A. Habraken and P. Teuffel, "Seismic control performance of a 3-story frame prototype equipped with semi-active variable stiffness and damping structural joints," *Earthquake Engineering & Structural Dynamics,* vol. 50, no. 13, pp. 3379-3402, 2021.

[11] F. Ruess, J. Schaenzlin and H. Benaroya, "Structural design of a lunar habitat," *Journal of Aerospace Engineering,* vol. 19, no. 3, pp. 133-157, 2006.

[12] H. Qi, M. Yang, X. Zhang, Y. Zhang, B. Wu and J. Liu, "Review on the structural design and materials of covers for inflatable lunar habitat (in Chinese)," *SPACECRAFT ENVIRONMENT ENGINEERING,* vol. 38, no. 6, pp. 715-722, 2021.

[13] C. Cassapakis and M. Thomas, "Inflatable structures technology development overview," *Space programs and technologies conference,* p. 3738, 1995.

[14] H. Benaroya, "Lunar habitats: A brief overview of issues and concepts," *Reach,* vol. 7, pp. 14-33, 2017.

[15] M. Schenk, A. D. Viquerat, K. A. Seffen and S. D. Guest, "Review of inflatable booms for deployable space structures: packing and rigidization," *Journal of Spacecraft and Rockets,* vol. 51, no. 3, pp. 762-778, 2014.

[16] J. Lin, C. Knoll and C. Willey, "Shape memory rigidizable inflatable (RI) structures for large space systems applications," in *47th AIAA/ASME/ASCE/AHS/ASC Structures, Structural Dynamics, and Materials Conference 14th AIAA/ASME/AHS Adaptive Structures Conference 7th*, 2006.

[17] Y. Liu , H. Du, L. Liu and J. Leng, "Shape memory polymers and their composites in aerospace applications: a review," *Progress in Materials Science,* vol. 56, no. 7, pp. 1077-1135, 2011.

[18] D. K. Kaja, Design of inflatable lunar structure, Rutgers The State University of New Jersey, School of Graduate Studies, 2017.